SCIENCE CHINA
Earth Sciences

• RESEARCH PAPER •

May 2016 Vol.59 No.5: 1025–1040
doi: 10.1007/s11430-016-5272-1

Dextral strike-slip of Sanguankou-Niushoushan fault zone and extension of arc tectonic belt in the northeastern margin of the Tibet Plateau

LEI QiYun[1,2*], ZHANG PeiZhen[1], ZHENG WenJun[1], CHAI ChiZhang[2], WANG WeiTao[1], DU Peng[2] & YU JingXing[1]

[1] *State Key Laboratory of Earthquake Dynamics, Institute of Geology, China Earthquake Administration, Beijing 100029, China;*
[2] *Earthquake Administration of Ningxia Hui Autonomous Region, Yinchuan 750001, China*

Received July 27, 2015; accepted January 15, 2016; published online February 24, 2016

Abstract The kinematic characteristics of the Sanguankou-Niushoushan fault (SGK-NSSF) are of great significance to the understanding of the extension of the arc tectonic belt in the northeastern margin of the Tibet Plateau. Using field surveys and various data collection methods, including large-scale geological mapping, measurement of typical topographies, and dating of sedimentary strata, it was determined that the SGK-NSSF exhibits obvious dextral strike-slip characteristics and thus is not a sinistral strike-slip fault, as believed by previous researchers. The results of this study show that the geological boundaries for the Paleozoic, Mesozoic, and Cenozoic eras were all dextrally dislocated by the fault, with the faulted displacements being similar. The maximum strike-slip displacement of the fault, after elimination of topographic effects, was found to be 961±6 m. The Sanguankou fault at the northern section exhibits obvious characteristics of more recent activities, with a series of small gullies having undergone synchronized dextral writhing after traversing the fault. The average horizontal slip rate of the fault since the late Quaternary was determined to be approximately 0.35 mm/a. The pre-existing fold structures formed during the late Pliocene were dislocated by the fault and became *ex situ*, indicating that dextral strike-slip of the fault could not have occurred prior to the late Pliocene. The maximum displacements and average slip rates were used to estimate the onset time of the dextral strike-slip activities of the fault as being after 2.7 Ma. In this study, the understanding of previous researchers concerning the extension in the northeastern margin of the Tibet Plateau was combined with analyses of the successive relationships between fold deformations and fault activities. This led to the finding that the extension in the northeastern margin of the Tibet Plateau reached the vicinity of the SGK-NSSF during the late Pliocene (~2.7 Ma), causing regional uplift and fold deformations of the strata there. During the early Quaternary, the northeastern compression of the Tibet Plateau and the counterclockwise rotation of the Ordos block collectively resulted in the dextral strike-slip activities of the SGK-NSSF. This then formed the foremost margin of the arc tectonic belt extension in the northeastern margin of the Tibet Plateau.

Keywords Northeastern margin of Tibet Plateau, Sanguankou-Niushoushan fault, Dextral strike-slip, Tectonic interactions between blocks, Arc tectonic belt

Citation: Lei Q Y, Zhang P Z, Zheng W J, Chai C Z, Wang W T, Du P, Yu J X. 2016. Dextral strike-slip of Sanguankou-Niushoushan fault zone and extension of arc tectonic belt in the northeastern margin of the Tibet Plateau. Science China Earth Sciences, 59: 1025−1040, doi: 10.1007/s11430-016-5272-1

*Corresponding author (email: leiqy624@163.com)

1. Introduction

The SGK-NSSF located at the composite junction of the Tibet, Alxa, and Ordos blocks (Figure 1), occupies a very important tectonic location (Deng et al., 2003; Zhang et al., 2003, 2013). Studies of this fault are of great significance in terms of not only understanding the extensional process of the arc tectonic belt in the northeastern of the Tibet Plateau, but also studying the effects of plateau extension on the tectonics of adjacent regions.

Some previous studies have been based on the premise that the SGK-NSSF is connected to eastern Luoshan fault to the south and is obliquely connected to the en echelon right step of the western Helanshan fault to the north. The SGK-NSSF was considered as a left-lateral strike-slip fault during the late Pleistocene because of some gullies exhibiting sinistral strike-slip motion (RGAFSAO, 1988; IGCEA, 1990; Chai et al., 2011; Wang et al., 2013a). Other researchers have assumed that the alignment of the SGK-NSSF changes to an east-west orientation at Yuanshanzi or Jijingzi to the north, connecting with the Chahanbulage fault to the west, and eventually extended to southern Longshoushan fault (Huo et al., 1989; Tang et al., 1990; Li, 1992; Zhang et al., 2004, 2010).

However, the latest research suggests that the Helishan fault and Longshoushan fault, located on the northern side of the Hexi Corridor, are thrust fault and these faults are the leading margin of the plateau extension toward the northeastern direction (Zheng et al., 2013a, 2013b). Significant kinematic differences lie between these faults and the SGK-NSSF. Furthermore, the discovery that the eastern Luoshan fault had dextral strike-slip characteristics led to the view that it is not connected to the SGK-NSSF to the north (Min et al., 1992, 2003). Different opinions remain concerning the geometric structure of the SGK-NSSF and the direction of its extension. There is also no conclusive evidence of the active age and the kinematic characteristic of this fault.

The arc tectonic belt in the northeastern margin of the Tibet Plateau is actually the leading edge of a plateau extension toward the northeastern direction (Molnar et a1., 1975; Tapponnier et a1., 1982, 2001; Deng et al., 1984; England et a1., 1985, 1997; Peltzer et al., 1989; Zhang et al., 2004). Many studies have been conducted on the extension and deformation of this arc tectonic belt during the late Cenozoic (Deng et al., 1989; IGCEA et al., 1990; Burchfiel et al., 1989, 1991; Zhang et al.,1988, 1990, 1991; Chai et al., 1998; Zheng et al., 2006; Li et al., 2009; Zheng et al., 2009,

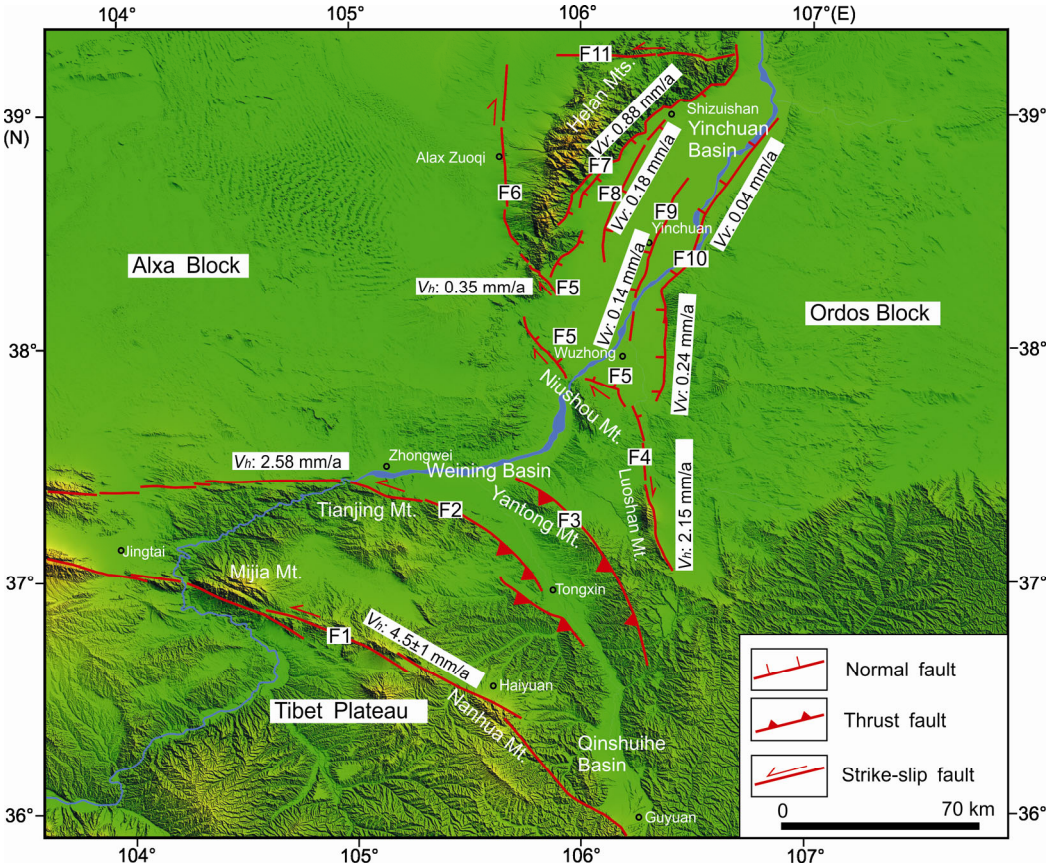

Figure 1 Distribution of faults within the arc tectonic belt in the northeastern margin of the Tibet Plateau and adjacent areas. F1, Haiyuan fault; F2, Tianjingshan fault; F3, Yantongshan fault; F4, Eastern Luoshan fault; F5, SGK-NSSF; F6, Western Helanshan fault; F7, Eastern Helanshan fault; F8, Luhuatai concealed fault; F9, Yinchuan concealed fault; F10, Huanghe fault; F11, Zhengyiguan fault.

2013b; Wang et al., 2013b, 2014; Shi et al., 2013; Zhang et al., 2015). These studies focused mostly on the Haiyuan fault and Tianjingshan fault, however, few studies have been conducted on the outermost SGK-NSSF, and these have been limited to indirect inferences of its evolutionary processes from the interpretations of seismic profiles (Wang et al., 2013a; Chen et al., 2013). There is a lack of detailed research on the tectonic evolutionary processes as reflected by the fault itself, as well as the Cenozoic stratum in its vicinity. This has prevented a complete understanding of the extension undergone by the arc tectonic belt in the northeastern margin of the Tibet Plateau.

In this study, field surveys, including the detailed geological and geomorphological mapping, OSL dating on alluvial surfaces, were conducted to identify the geometric distribution, kinematics of the fault zone, and estimation on slip rates along the SGK-NSSF. Concrete evidence suggests that the SGK-NSSF is a dextral strike-slip fault. Meanwhile the maximum strike-slip displacements and the average strike-slip rates during the late Quaternary were determined. These findings could well change the current understanding of the arc tectonic belt extension in the northeastern margin of the Tibet Plateau.

2. Regional tectonic environment and geometric distribution of faults

The arc tectonic in the northeastern margin of the Tibet Plateau is located to the south of the SGK-NSSF zone. It is formed by the Haiyuan fault, Tianjingshan fault, and Yantongshan fault from south to north. Among them, the Haiyuan fault is the main fault which underwent different tectonic deformations, i.e., from extrusion by thrusting that began from approximately 8–10 Ma to a sinistral strike-slip motion at 5.4 Ma (Zheng et al., 2005, 2006; Wang et al., 2013a, 2014). The maximum strike-slip displacement was 14 km which was absorbed by the fold deformation and thrust fault located at the end portion of the fault (Deng et al., 1989; IGCEA et al., 1990; Zhang et al., 1991; Burchfiel et al., 1991). The average slip rate during the late Quaternary was approximately 4.5±1 mm/a (Li et al., 2009; Zheng et al., 2013b). In 1920, an 8.5 magnitude earthquake occurred above the fault in Haiyuan County (IGCEA et al., 1990).

The Tianjingshan fault had similar tectonic evolutionary stages and a similar transformation mode (Zhang et al. 1988, 1990, 1991; Zhang et al., 2015). However, thrusting and sinistral strike-slip there began later, at approximately 5.4 Ma and 2.6 Ma, respectively (Wang et al., 2013b). The maximum horizontal displacement was 3.2 km, while the average slip rate during the late Quaternary was 2.29–2.86 mm/a (Chai et al., 1998; Li, 2005). In 1709, a 7.5 magnitude earthquake occurred in Zhongwei City (IGCEA et al., 1990). The smaller-scaled Yantongshan fault began thrusting at approximately 2.6 Ma. There was no obvious activity there during the Quaternary, with the most recent activities having occurred during the middle of the late Pleistocene (IGCEA et al., 1990; Wang et al., 2013b).

The Yinchuan graben is located to the north of the SGK-NSSF zone. Formed by a group of four normal faults, it consists of a Cenozoic stratum with thick sedimentation. The northern and southern sections of the basin consist of two half-grabens of opposite polarities, while the structure in the middle section is that of a graben within a graben (Yan et al., 2002). The Cenozoic stratum is thick at the north but thin at the south, with subsidence at the center deviating from west to east. The maximum thicknesses of the Cenozoic and Quaternary strata are 7000 m and 1600 m, respectively (RGAFSAO, 1988; Li, 1992).

Eastern Helanshan fault forms the western boundary of the basin and separates Helanshan from the Yinchuan Basin. Intense activities causing rapid tilting and uplifting of Helanshan occurred there during 10–12 Ma (Liu et al., 2010). Activities have remained intense since the late Quaternary, with a vertical slip rate of approximately 0.88 mm/a (RGAFSAO, 1988). In 1739, an 8.0 magnitude earthquake occurred above the fault in Pingluo County, with the maximum vertical coseismic displacement of 4.4 m (Deng et al., 1996).

The eastern boundary of the Yinchuan Basin is demarcated by the Huanghe fault. During the late Quaternary, activities were weak at the northern section of the fault. The vertical slip rate was 0.04 mm/a, compared to 0.24 mm/a for the southern section (Liao et al., 2000; Lei et al., 2013). The vertical slip rate of the Yinchuan concealed fault was 0.14 mm/a during the Holocene (Lei et al., 2008). The northern section of the Luhuatai fault was a Holocene active fault at a vertical slip rate of 0.18 mm/a. However, the southern section has been inactive since the late Pleistocene (Lei et al., 2011).

Field surveys have confirmed that the SGK-NSSF zone is connected to eastern Luoshan fault to the south and is obliquely connected to the western Helanshan fault to the north in an en echelon right step. The fault is formed by three discontinuous secondary faults from south to north, namely, Guanmahu fault, Liumugao fault, and Sanguankou fault (Figure 2).

The Guanmahu fault is the boundary between the Yinchuan Basin and the alluvial terraces of the Niushou Mountain northeastern piedmont. The topographic variations were originally significant, but the entire section has been severely modified by artificial interventions. Denudation and cutting of the topographic units are obvious, and the original geomorphological surfaces no longer exist. Trenches revealed that the fault dip toward the northeast with a component of normal motion.

The Liumugao fault, similarly, tends toward the northeast. The topographies on its two sides are significantly different. A number of large gullies traverse the fault zone and are

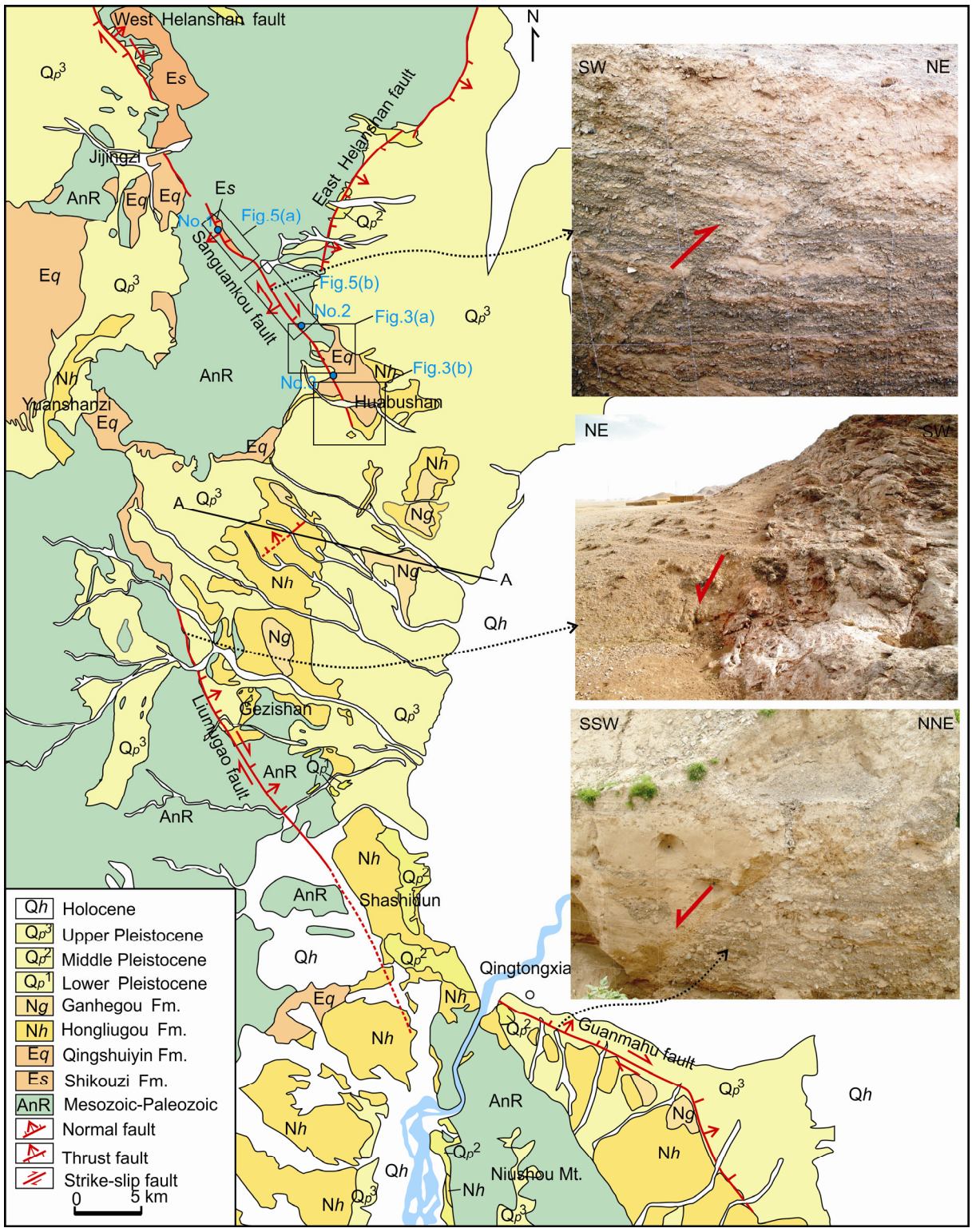

Figure 2 Geometric distribution of the SGK-NSSF.

offset by right-lateral strike-slip motion with a reverse component. The Sanguankou fault cuts through the mass of Helan Mountains obliquely and expresses as a clear linear feature. Young fault scarps developed that truncated dislocation of gullies along the fault. The geological boundaries have undergone dextral dislocation in several places. The fault dips toward the southwest and exhibits both dextral strike-slip and thrusting motion.

Previous researchers believed that a Quaternary active fault existed within northeastern piedmont of the Niushou

Mountain (IGCEA, 1990). Previous studies showed that the scale of the fault was small and that it had only developed bedrock scarps approximately 4 km in length near the vicinity of Jiuquan. The extensions at both ends were capped by early Pleistocene alluvial gravels that had undergone calcareous cementation. There is no evidence of development of a scarp topography. The Hongliugou Formation overlies the Ordovician System directly and has consistent stratigraphic occurrences. Industry profiles obtained for oil and seismic exploration across the Niushou Mountain do not indicate the existence of this Quaternary fault (Wang et al., 2013a). Hence, it can be concluded that the northeastern Niushoushan fault is small in scale, only partially developed, and not an active fault.

To the further south, Eastern Luoshan fault continues to extend with an almost north-south orientation. It is obliquely connected to the en echelon left step of the Guanmahu fault near the Yinchuan Basin, but does not connect to the Huanghe fault. The dextral strike-slip motion along the eastern Luoshan fault is obvious, with an average slip rate of about 2.15 mm/a during the late Quaternary (Min et al., 2003).

3. Geological and geomorphological evidence for dextral strike-slip of the SGK-NSSF zone

3.1 Dextral dislocations of geological boundaries

The geomorphological evidence for strike slip of the SGK-NSSF zone is most clearly exhibited by the Sanguankou fault at the northern section. The geomorphology of the other two sections has not been well preserved because the fault zone did not cut deeply into the stratum and heavily modified by human being. For the Sanguankou fault, dextral dislocation occurred at three stratigraphic boundaries belonging to different geological ages. Following is a summary of the boundary characteristics of the faulted stratigraphic units that were listed in chronological order.

3.1.1 Dextral dislocation at the boundary between the Ordovician sandstone and limestone

The Sanguankou fault cuts through the middle Ordovician Pingliang Formation at its southern section near Gaoshidun (Figures 3a, 4a). The boundaries between the upper and lower sections of the formation underwent dextral dislocation, which is the conformity contact relationship. The lithology of the lower section consists of greyish green thin layer fine-grained feldspathic sandstone, and that of the upper section is grayish argillaceous limestone (NBGMR, 1990). The measured occurrence of the fault plane is 230°∠75°. The occurrence of the limestone subface on the west side of fault is 150°∠30°, while that of east side of fault is 170°∠36°. The interface of the formation intersects with the fault at a wide angle of 60°–80°.

After traversing the fault, the boundary shows an obvious deviation to the right. The breakpoints are clearly exposed above the surface, reflecting a dextral-lateral strike-slip motion occurred on the fault. Using large-scale geological mapping, it was determined that the dislocation at this boundary resulted in a displacement of approximately 1.1 km. A 90 m fall between the two breakpoints was measured using a Differential Global Positioning System (DGPS). This is not the actual displacement because of the impacts of terrain and occurrence. A calibration method was used to calculate the stratigraphic occurrences of the two plates separately (Figure 3c). The displacements were 965 m and 946 m, so the average value of 955 m was adopted.

3.1.2 Dextral dislocation at the boundary between the Ordovician limestone and Cretaceous conglomerates

This is located to the south of the previous boundary, with unconformity contact relationship (Figure 4b). The Cretaceous System consists of purplish red conglomerates and belongs to the subgroup below the Cretaceous Miaoshanhu Group (NBGMR, 1990). The occurrences of the Cretaceous conglomerates in the both plates of the fault keep consistent (Figure 3a). This boundary spreads continuously on both sides of the fault but is disrupted where it traverses the fault, causing it to deviate to the right. A similar deviation of the overall limestone and conglomerate strata occurs at the same location, indicating dextral strike-slip displacement of the fault. The general direction of this boundary is similar to that of the previous boundary. The former also intersects with the fault at a wide angle. The breakpoints of the western side of the fault are clearly exposed, indicating a folding surface steepening into deep (Figure 4b). Because the eastern side is covered by the Cenozoic stratum, this boundary is not exposed near the fault. The nearest outcrop is approximately 500 m to the east of the fault. Projecting this point onto the fault zone along the strike of the stratum, a dextral displacement of 1.4 km was calculated.

Furthermore, the Ordovician limestone outcrop in the vicinity of the fault is also clearly visible. Using the limestone mass as a reference, it was determined that the Ordovician stratum had been displaced by at least 1.14 km. Given the huge interval between sedimentation by the Ordovician and Cretaceous Systems, as well as the complexity of the original topography of the Cretaceous stratum, the contact boundary of the two systems might be not a simple plane. Both topographical changes and differences in denudation have affected the outcrop location of this boundary. Thus, the measured displacements might be greater than the actual values. On the other hand, the displacements determined using the Ordovician limestone rock mass as a reference might be closer to the actual values.

3.1.3 Dextral dislocation at the boundary between the Qingshuiying Formation mudstone and Hongliugou Formation conglomerates

The boundary between the Qingshuiying Formation and

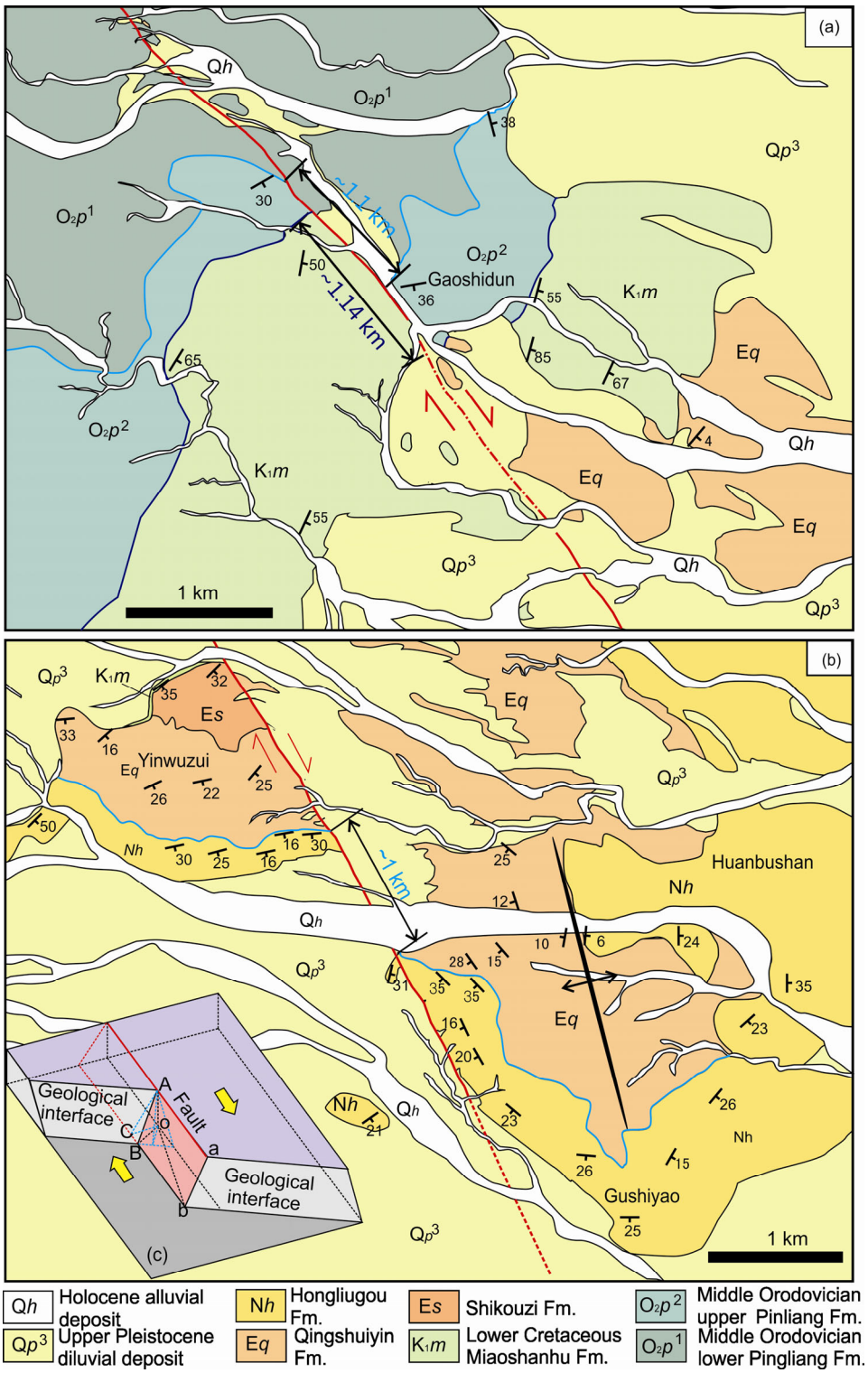

Figure 3 Geological map of dislocations in the Sanguankou fault. (a) Gaoshidun region; (b) Huabushan region; (c) Schematic diagram of the fault slip effect. Site A and b are breakpoints on the ground; line ob is the distance between the two breakpoints as projected onto the horizontal plane; and line Aa and Bb refers to actual dislocation of the stratum.

Hongliugou Formation is disconformity and located at the southeastern end of the Sanguankou fault, near Xiaoshitou (Figure 4c, d). The Qingshuiying and Hongliugou formations consist of brownish red mudstone and grayish conglomerates, respectively. Both strata form the western flank of the Huabushan anticline at this location, with the fault cutting through them. This boundary deviates to the right along the consequent fault zone, indicating that the fault has

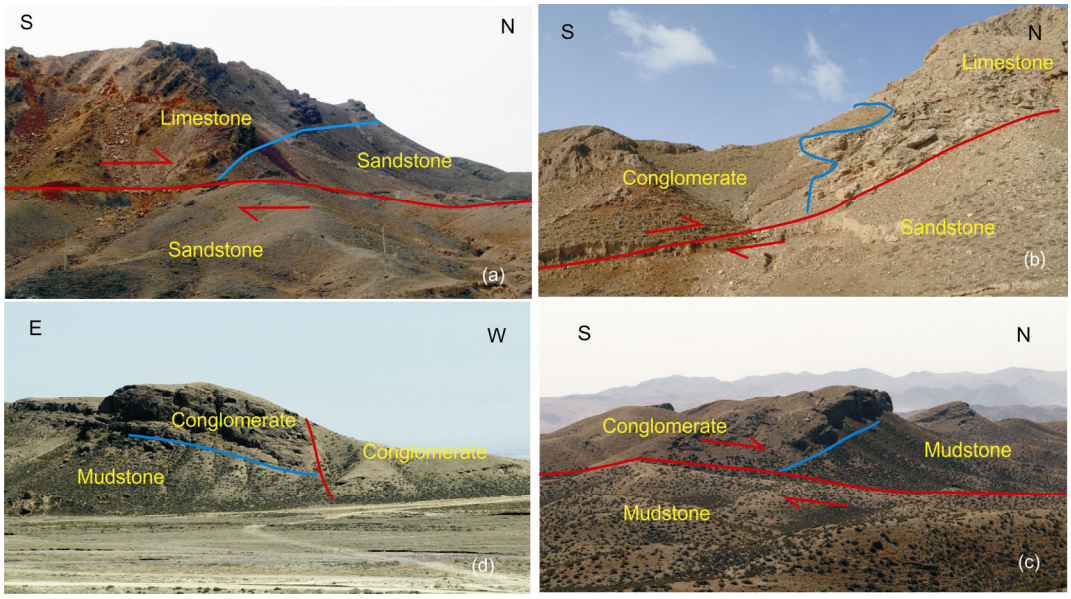

Figure 4 Photographs of geological boundaries near the Sanguankou fault. (a) Boundary between the Middle Ordovician sandstone and limestone at the west side of the fault; (b) boundary between the Middle Ordovician limestone and Lower Cretaceous conglomerates at the west side of the fault; (c), (d) boundaries between Qingshuiying Formation mudstone and Hongliugou Formation conglomerates at the west side and east side of the fault, respectively.

dextral strike-slip characteristics (Figure 3b). The measured occurrence of the bottom of the conglomerate unit at the western plate of the fault is 170°∠30°. The occurrence of the eastern plate is 225°∠35°, while that of the fault is 250°∠75°. The breakpoints are exposed clearly on both plates of the fault, with a height differential of 15 m. The distance between the two breakpoints, measured using the large-scale geological map, is 1 km. A mapping calculation was performed separately using the same method to determine more realistic displacements based on different occurrences. The displacements calculated were 977 m and 957 m, so the average of 967 m was adopted.

In summary, the fault dislocated the Paleozoic, Mesozoic, and Cenozoic stratigraphic boundaries, with the displacements for all three being almost 1 km. These displacements indicate that dextral dislocation by the fault occurred after sedimentation of the Hongliugou Formation and that dextral strike-slip was sustained after activities had begun. There is no evidence for any occurrence of sinistral strike-slip movements. Among the three boundaries, the interface between the Ordovician and Cretaceous Systems is undulating and complex in form. As a result, topographic heights and differences in denudation were concluded to have had a greater impact on the outcrop location of the boundary. Because it is difficult to reestablish the locations of the breakpoints on both sides of the fault based on stratigraphic occurrences, the displacements were used solely for reference, and no further calibration was carried out. However, the other two interfaces were planar. The horizontal displacements after calibration were 955 m and 967 m. Because these two values are very similar, an average value of 961± 6 m was adopted. This may be a more reliable value for the maximum horizontal strike-slip displacement of the Sanguankou fault.

3.2 Dextral dislocation of present-day gullies

The Sanguankou fault cuts through Helan Mountains obliquely. Its topographic trails are clear, and the linear characteristics are obvious. The topographies on the two sides of the fault are significantly different: the southwestern plate is a mountainous area of exposed bedrock, while some small-scale alluvial fans are found near the fault trace. A series of gullies along the fault underwent synchronized dextral writhing (Figure 5a, b). The locations at which the gullies were offset are mainly in the extension direction of the fault scarp at the surface. The fault planes are also exposed on both walls of the gullies, indicating the dextral writhing of the gullies are resulted from dislocation of the fault (Figure 5c).

The erosive forces of some larger gullies were stronger, and these quickly expanded into fans after passing through the Sanguan. The river channels were also unstable and changeable. Therefore, most of these do not exhibit any characteristic of dextral dislocation. Instead, it is more easy for smaller gullies that developed on the alluvial fans to retain dislocation by the fault. These are most obvious within a 10 km range of the fault between the Gaoshidun and Sanguankou. A portable rangefinder was used for statistical measurements of 42 small gullies along this section that exhibit obvious dextral dislocation. DGPS was used for measurements at some sites. The distribution of the displacements is shown in Figure 5d. The results showed that most dislocations involved minor displacements within two

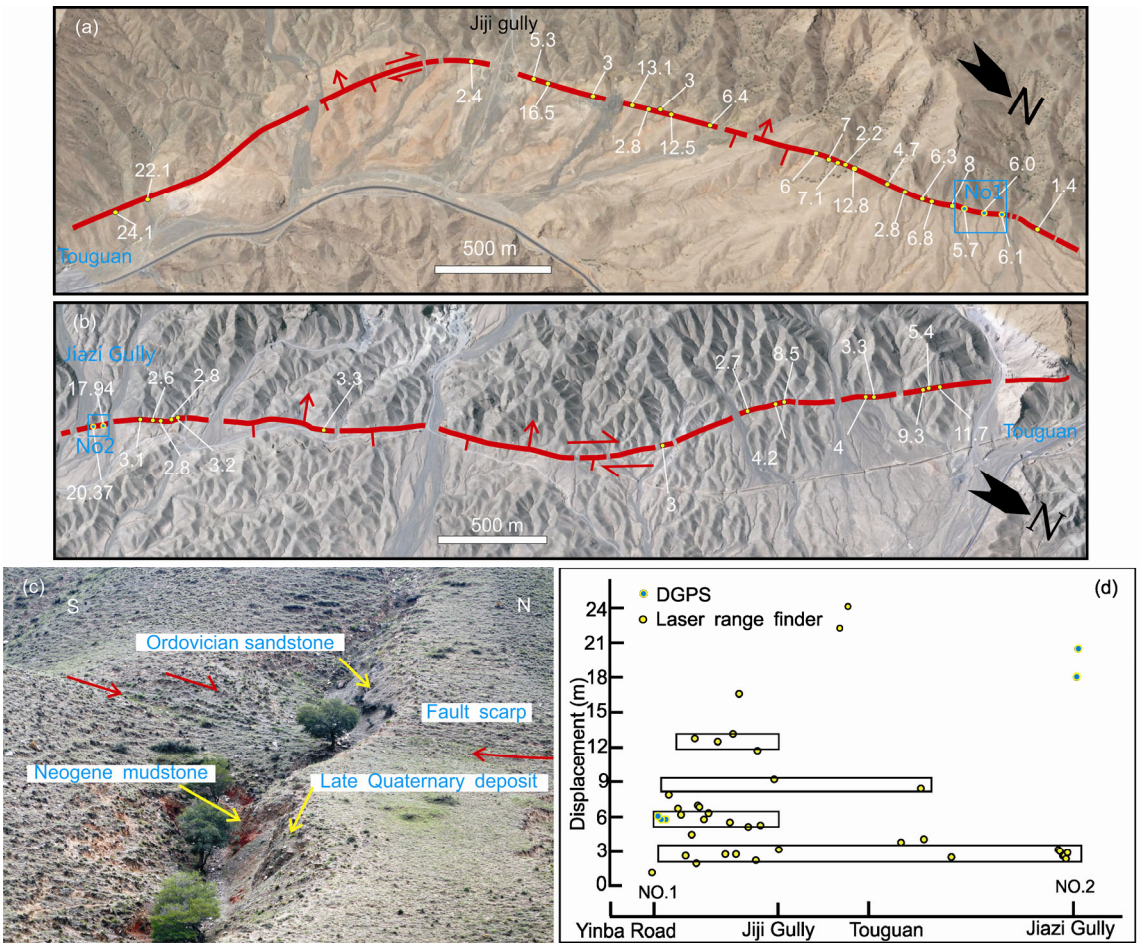

Figure 5 Dislocation of gullies along the Sanguankou fault. (a), (b) Location maps of gullies (measured); (c) typical dextral dislocation of gully; (d) distribution diagram for the dislocations of various gullies.

classes of 3 and 6 m. The individual displacements were distributed around 9, 12, and 15 m. The displacements at 3 and 6 m along the fault were closely and alternately distributed. The developmental scale of the gullies shows that the displacements in the 6 m tranche cut deeper than those in the 3 m tranche. The former is also of a larger scale and was developed earlier. Studies on fault mechanics and modern seismology have found that the distribution of displacements for a single rupture tend to be in a smooth arc, with rapid attenuation at both ends of the fault (Scholz, 2002; Xu et al., 2008). A wavelike distribution with alternatively large and small displacements is rare. Thus, displacements in the 3 m and 6 m tranches were not formed simultaneously during the same earthquake. The former corresponds to dislocations and displacements caused by the most recent earthquake, while the latter corresponds to dislocations caused by two earthquakes. Based on this finding, it was determined that the horizontal coseismic displacement of the Sanguankou fault was approximately 3 m.

In the vicinity of the Sanguan (No. 1), three small adjacent gullies that straddle the fault underwent synchronized dextral writhing (Figure 6). The three gullies are of similar size, with depths and widths of approximately 2 and 4 m, respectively. These extend for less than 2 km upstream toward the mountainous bedrock area. After passing through the col, these cutting through the alluvial fans of the same era traverse the entire fault zone, deviate to the right, and then intersect downstream to form a single gully. DGPS was used to measure and prepare a topographic map of the surrounding areas. Among the three gullies, the phenomenon of dextral dislocation was best preserved by the north gully. With the exception of the southern wall near the fault, which had been partially eroded, the extension of this gully is generally linear and better reflects dextral dislocation by the fault. Using the center line of the gully as a reference, the measured displacement was determined to be 6.1±0.4 m.

The south gully deviates not far downstream, after having traversed the fault zone. The length of extension, which is similar to that of the preserved gully upstream, was less than 20 m. The measured displacement was 5.9±0.6 m with respect to the center line of the gully. The overall deviation of the middle gully downstream was large, but this was not due to dislocation caused by the fault. Careful observations found the small residual terraces of this gully near the fault

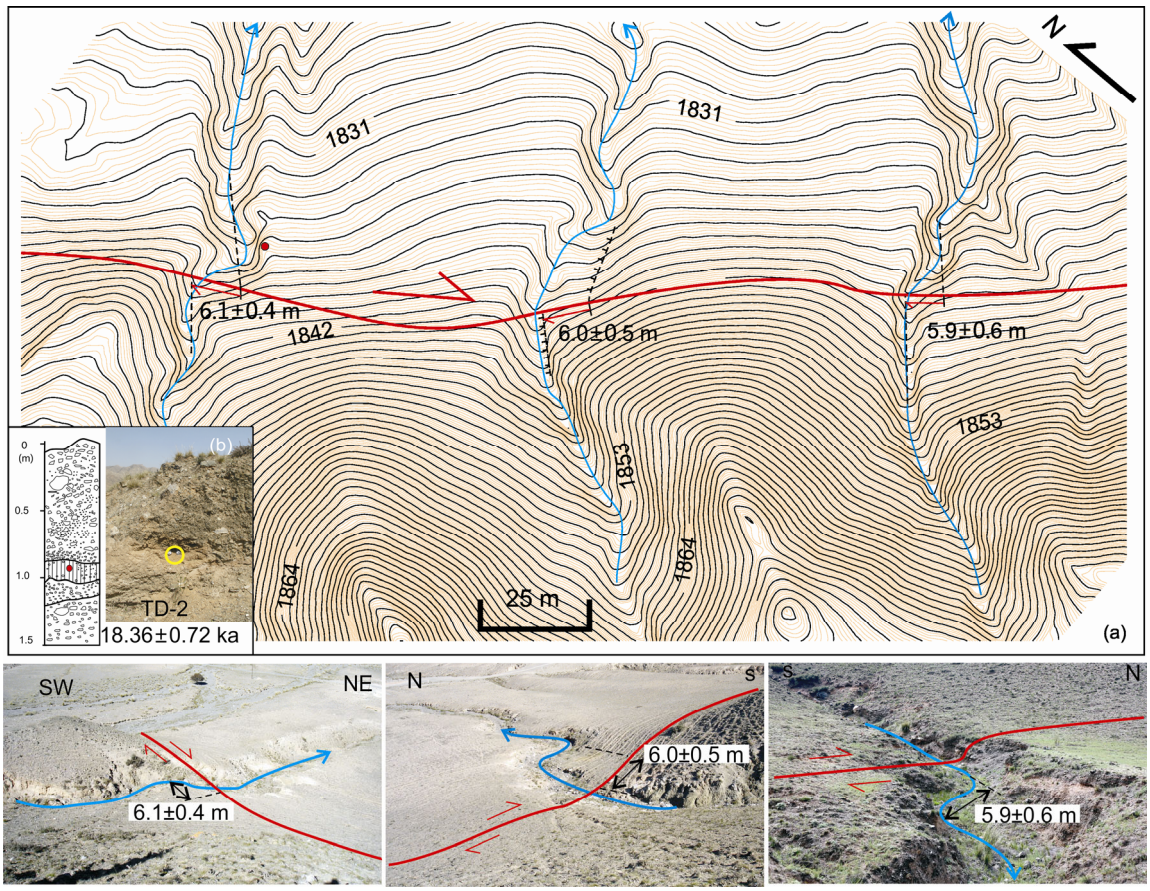

Figure 6 Measured dislocation of gully near Sanguan (No. 1).

zone. The edges of the small terraces and alluvial fans have been preserved and remain intact, and they make up the early wall of the gully.

By comparing the southern walls of the gullies on both sides of the fault zone, the displacement was determined to be 6±0.5 m. The OSL sample TD-2 was collected from the southern wall of the north gully, approximately 1 m below the surface. The age was determined to be 18.36±0.72 ka (Figure 6b, Table 1). Hence, the gully must have been formed later. The displacements and the results of the dating of the three gullies were used to estimate their respective horizontal slip rates as 0.33±0.025, 0.32±0.035, and 0.33±0.033 mm/a.

At the southern bank of the north tributary of Jiazi gully (No. 2), fault scarps developed above the T3 terrace. Ordovician sandstone is exposed on the southern wall of the upstream gully. It is overlain by alluvial gravels and has a thickness of approximately 1 m. The gully wall deviates to the right at the fault zone. A wide gully that was similarly dislocated dextrally (Figure 7a) developed to the south. Detailed measurements obtained using DGPS show that the displacements of the south gully wall and the center line of the gully are quite similar, at 17.9±1 m and 20.3±3 m, respectively. A pit was excavated downstream of the T3 terrace, and OSL sample TD-6 was collected from 0.5 m beneath the surface. The age was determined to be 54.88±4.1 ka (Figure 7b, Table 1). The dating results and calculated displacements were used to determine two average horizontal slip rates for the fault: 0.33±0.030 and 0.37±0.061 mm/a, respectively.

At north Yingzuishan (No. 3), the T4 alluvial mesa remains between the two large gullies, with the fault zone dislocating the mesa and forming a vertical scarp reaching a height of 8 m. The gully within the mesa that traverses the fault zone underwent synchronized dextral dislocation, together with the northern and southern edges of the mesa. DGPS measurements were obtained at all three dislocations (Figure 8a). The gully within the platform traverses the fault zone upstream and then bifurcates into two tributaries. The depth of undercutting and the length of the extension by the south tributary are both greater than that by the north tributary. Under the condition of similar lithology, the south tributary was formed earlier, while the north tributary evolved during a later stage of development. Therefore, displacement of the center line of the south tributary was used as a reference when comparing measurements upstream. The measured displacement was 35.6±2 m.

Using the locations of the northern and southern edges of the mesa on both sides of the fault as references, the measured displacements at the two edges were 52.4±5 m and

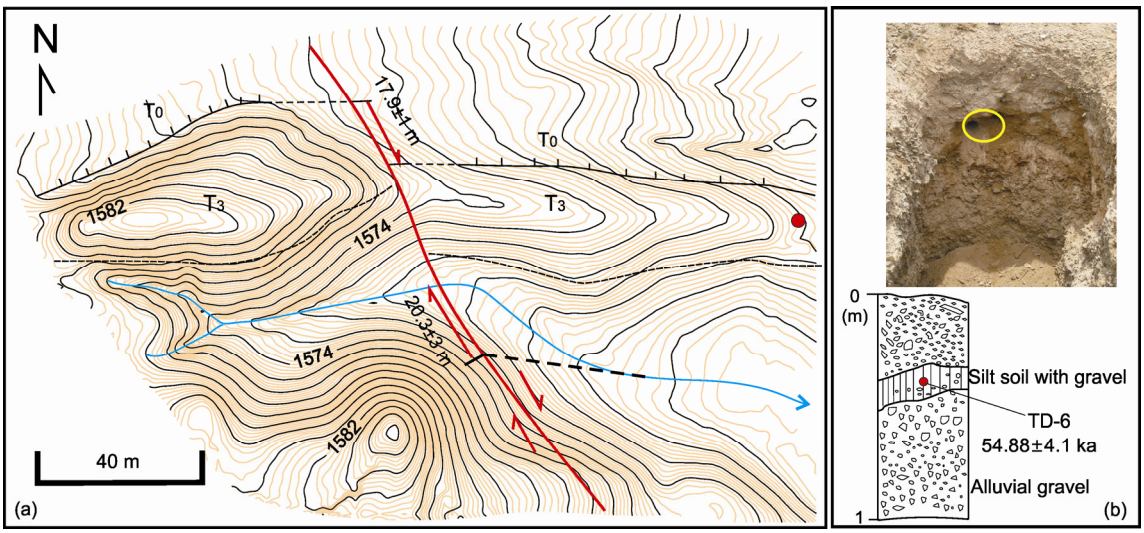

Figure 7 Measured cross-sectional view of Jiazi gully (No. 2).

Table 1 Dating results of OSL samples[a)]

Sample No.	Depth (m)	U (ppm)	Th (ppm)	K (%)	Moisture content (%)	Equivalent dose (Gy)	Dose rate (Gy/ka)	Age (ka)
TD-2	1	2.60	10.26	2.16	10±5	65.88±1.03	3.59±0.13	18.36±0.72
TD-6	0.4	2.29	11.09	2.20	10±5	197.74±12.87	3.60±0.13	54.88±4.10
TD-7	1	2.78	6.58	1.24	10±5	306.26±21.88	2.44±0.08	125.36±9.85

a) Tested by the Luminescence Laboratory, Institute of Earth Environment, Chinese Academy of Sciences.

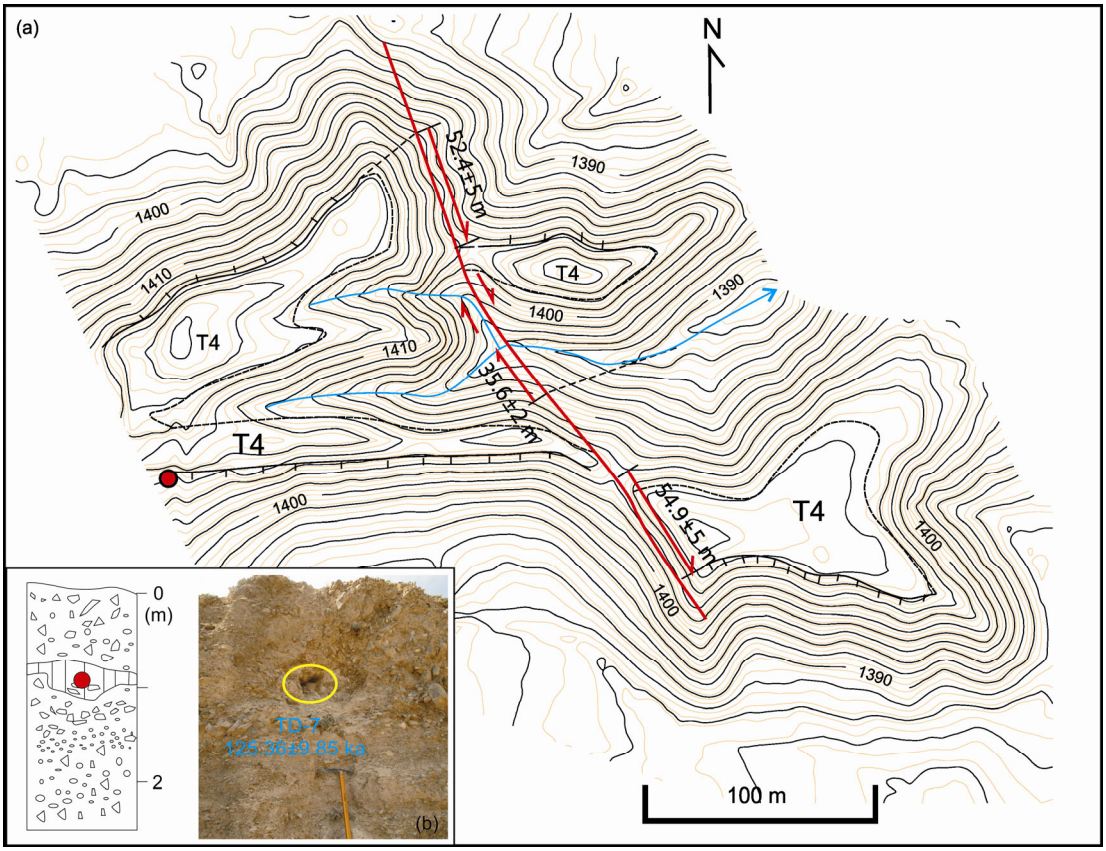

Figure 8 Measured geomorphology of northern Yingzuishan (No. 3).

54.9±5 m, respectively. A natural section located 1 m from the surface is exposed at the southern edge, upstream of the mesa. Sandwiched within the layer of alluvial gravels is a layer of sand clay lenses. OSL sample TD-7 was collected from the layer, and dating resulted in an age estimate of 125.36±9.85 ka (Figure 8b, Table 1). The three aforementioned dextral displacements were divided by this age to obtain the following respective slip rates of the fault at this location: 0.28±0.027, 0.42±0.052, and 0.44±0.053 mm/a.

Eight average slip rates were estimated using the eight displacement values and the test results for the three OSL samples, all of which were obtained from the three aforementioned measurement points. Because the gullies at the three survey points and the boundaries of the geomorphic surface margins all developed after the formation of the alluvial fan (or mesa surface), while the samples tested were from sedimentations underneath the alluvial fan (or mesa surface), the samples can be considered to correspond to a period prior to the era in which the alluvial fan (or mesa) was formed. Hence, the estimated age should be greater than that suggested by the era during which the dislocations occurred, while the slip rates obtained should be smaller than the actual rates. All eight average slip rates obtained represent the minimum slip rates of the fault. Overall, it can be seen that the eight rates derived from various displacements and periods are quite close and belong within the same numerical order. An average value of 0.35±0.040 mm/a was adopted for the displacements.

Paleoseismic research shows that the interval for ancient earthquake recurrence at the Sanguankou fault was approximately 8000–10000 a (this will be discussed in a separate paper), while the coseismic horizontal displacement was 3 m. Based on these values, a preliminary estimate of the slip rate would be 0.3–0.38 mm/a. This is close to the rate determined in this study and also matches the 6 m displacement of the gully at the measurement point near Sanguankou, which was caused by two earthquake dislocations and accumulated during 18.36 ka. As such, despite this study having been limited by objective conditions such that only the minimum slip rate of the Sanguankou fault was obtained, the finding was close to the actual slip rate. This indicates that the horizontal slip rate of the Sanguankou fault during the late Quaternary was slow, at approximately 0.35 mm/a.

4. Dextral strike-slip of fault and extension of arc tectonic belt in the northeastern margin of the Tibet Plateau

4.1 Onset time for dextral strike-slip of the SGK-NSSF

The Cenozoic stratum is widely distributed in Ningxia. Previous researchers divided it through comparison into the Sikouzi, Qingshuiying, Hongliugou, and Ganhegou formations, as well as the Quaternary System. Various studies had also been conducted to determine the absolute age of this stratum (Huo et al., 1989; NBGMR, 1990; Li, 1992; Shen et al., 2001; Jiang et al., 2007; Zhang et al., 2010; Wang et al., 2011). Among these, research on Sikouzi cross section, located in southern Ningxia, has been the most detailed and reliable. The confirmed stratigraphic ages of the various formations are as follows: Sikouzi (29–25.3 Ma), Qingshuiying (23.8–17 Ma), Hongliugou (17–5.4 Ma), Ganhegou (5.4–2.5 Ma), and accumulation of loose conglomerate from the Quaternary System (2.5–0.5 Ma) (Wang et al., 2011). That time scale was used in this study to determine the temporal limits for tectonic deformations within this region.

Large-scale geological mapping indicates that the Sanguankou fault dislocated the western flank of the Huabushan anticline (Figure 3b). This shows that deformation of the anticline and fault activities occurred during different periods and that the latter happened after fold deformation. The western flank of the Huabushan anticline was formed by the Hongliugou and Qingshuiying formations. However, the Ganhegou Formation, which is exposed to the south of the anticline, was also drawn into the fold deformation during the same period. No obvious angular unconformity between these formations was found during the field surveys (Figure 2). Seismic reflection profiles of the area south of Huabushan also clearly revealed that the Cenozoic stratum there has been fold (Figure 9). The profiles also showed that the Qingshuiying, Hongliugou, and Ganhegou formations were all drawn into the fold deformation, with the latter two being exposed on the surface. With the exception of the boundary between the Quaternary and the Ganhegou Formation, all other stratigraphic boundaries are clear with similar morphologies, and do not contain any angular unconformities. These suggest that fold deformations in this region were formed at least after deposition of the Ganhegou Formation.

Shallow seismic profiles did not reveal whether or not the Quaternary deposition had undergone deformation. However, within the study area, the following overlie the Neogene System in angular unconformity without exception: scattered alluvial conglomerates from the early Pleistocene that were cemented, alluvial sandy gravels from the middle Pleistocene distributed on both banks of the Yellow River, and alluvial materials from the late Pleistocene that are widely distributed on the piedmonts (Huo, et al., 1989; NBGMR, 1990). These indicate that fold deformations occurred prior to the Quaternary. In addition to the fold structures, the cross section also shows the development of a small-scale normal fault that cuts through the Qingshuiying and Hongliugou formations of the western flank of the anticline. The resolution of the images was limited to reveal whether dislocation occurred in the Ganhegou Formation and Quaternary deposits. An antithetic fault scarp was found to have developed on the surface where the fault extents upward. The fault scarp, striking along northeastern

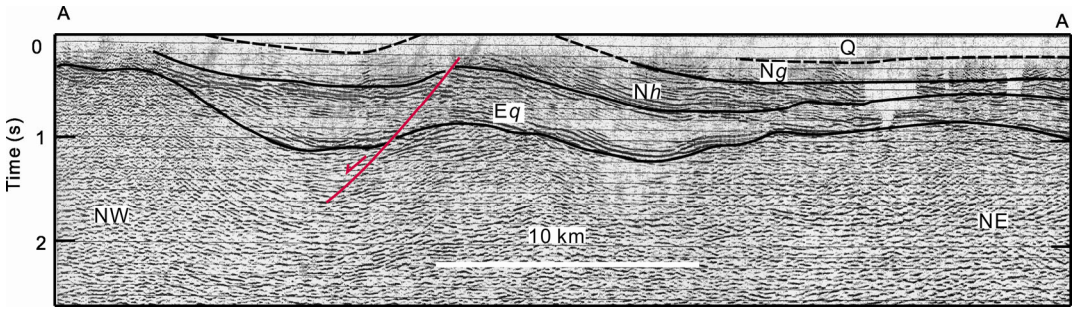

Figure 9 Shallow seismic profile of the Huabushan region.

direction, is approximately 300 m long and has dislocated the late Pleistocene alluvial fan (Figure 2). It would not be possible for the normal fault zone, which developed on one flank of a broad and gentle fold, to be a product of the same time as the fold deformation. Furthermore, activities of the normal fault zone occurred during the late Pleistocene, whereas the Quaternary System was not affected by fold deformation. These findings suggest that the normal fault zone in the cross section belongs to a different era from the fold and that its activities occurred subsequent to fold deformation. The spatial distribution of the fault indicates that the normal fault zone might have been caused by the pulling apart of the Sanguankou fault and Liumugao fault during dextral strike-slip. Thus, we infer that the SGK-NSSF underwent two periods of tectonic deformation. The stratum underwent fold deformation during the earlier period between the deposition of the Ganhegou Formation and the Quaternary System. During the later period, the fault underwent dextral strike-slip, accompanied by pulling apart locally, which resulted in the formation of the small-scale, secondary normal fault zone.

As mentioned previously, the fold deformation of the Sanguankou-Niushoushan region occurred in the period after deposition of the Ganhegou Formation, and the Quaternary System was not drawn into the deformation. Seismic reflection profiling shows that the Ganhegou Formation of the Huabushan region extends eastward into the Yinchuan Basin. Its top and bottom boundaries are continuous, while its thickness is smaller than that of the section in the basin (Figure 9). Subsidence of the Yinchuan Basin has been ongoing since the Cenozoic era, and sedimentation has continued during this time (Li, 1992). It seems not possible that the Ganhegou Formation has been eroded in the Yinchuan Basin. Thus, we infer that the Ganhegou Formation within the Huabushan region was also in a state of continuous sedimentation. The only difference was that its deposition rate was slower than that of the Yinchuan Basin. Because sedimentation of the Ganhegou Formation at the Sikouzi cross-section were dated back to 5.4–2.5 Ma (Wang et al., 2011), fold deformation in the Huabushan is believed to have occurred during the late Pliocene.

In addition, the maximum horizontal strike-slip displacement of the SGK-NSSF was 961 m, and the average slip rate was not less than 0.35 mm/a since the late Quaternary. Combined the maximum displacements with the average slip rate, the onset time of the slip was estimated to be approximately 2.7 Ma. Because the estimated slip rates belong to the lower limit, the dextral-strike slip of the fault should have commenced shortly after 2.7 Ma. On the other hand, fold deformation happened prior to dextral-strike slip of the fault, meaning that it was before 2.7 Ma. Regional stratigraphic correlation indicates that fold deformation occurred during the late Pliocene. Because there is no other more accurate and direct constraint for dating the tectonic deformations, it was inferred that there was a short interval between fold deformation and the fault strike-slip activities. Specifically, the fold deformation occurred around 2.7 Ma, whereas the fault dextral-strike slip might have occurred at the early Quaternary.

In summary, the vicinity of the SGK-NSSF has undergone two tectonic deformation processes. During the earlier period (the late Pliocene, close to 2.7 Ma), the main deformation was stratigraphic folding, which was manifested as shortening of the sub-blocks and regional uplift. During the later period (the early Quaternary), the process transformed to dextral-strike slip along the SGK-NSSF manifested as lateral extrusion of the sub-blocks.

4.2 Dextral strike-slip faulting of SGK-NSSF zone and extension of the arc tectonic belt

Deformation of the Cenozoic stratum in the vicinity of the SGK-NSSF had far-reaching impacts that were distributed from south to north continuously. These can be seen at the southern end of the Helan Mountains, including Huabushan, Miaoshanhu, and Gaoshidun, and at the eastern and western of the Niushou Mountain. The deformation is mostly in the form of wide, gentle folds or gently inclined monoclinic structures. The newest stratum to be drawn in was the Ganhegou Formation, while the Quaternary overlies the Neogene deposits with angular unconformity (Huo et al., 1989; NBGMR, 1990; Wang et al., 2013a; Liang et al., 2013). The axes of these folds are either in the northwest or north-northwest directions, indicating that they were compressed along the northeast-southwestern direction.

The Yinchuan graben is located to the northeast of the

fault zone, with the main structure being a normal fault zone lying in a northeastern direction. The thick Cenozoic stratum that was deposited within reflects sustained extension action in the southeastern direction (RGAFSAO, 1988; Chai et al., 2011). It is obvious that the compression in northwestern direction is incorporate with this extension structure in the northeastern direction. On the other hand, the Tibet Plateau is located to the southwest of the fault zone and continued to extend northeastward. Overall, both the arcuate fault that protrudes in a northeastern direction and the Cenozoic folds near the fault zone that are distributed in a northwestern direction reflect the compression related to the Tibet Plateau has grown into this fault zone (IGCEA et al., 1990; Zhang et al., 1990; Chai et al., 1998). Undoubtedly, the Cenozoic folds in the vicinity of the SGK-NSSF zone were the results of the extension and compression in the northeastern margin of the Tibet Plateau. Meanwhile, the dextral strike-slip of the SGK-NSSF zone could be due to adjustments in the conditions of the sub-blocks after they were being compressed.

The arc tectonic belt in the northeastern margin of the Tibet Plateau consists of several linear sub-blocks (IGCEA, 1990). In this study, the three major active faults, the Haiyuan fault, Tianjingshan fault, and SGK- NSSF, were used as dividers for these sub-blocks: Nanhuashan-Liupanshan, Xiangshan-Tianjingshan, and Yantongshan-Niushoushan (Figure 10). There were two periods of tectonic deformation at the boundaries of these sub-blocks and in the vicinity of the fault. Fault thrusting or fold deformation of the stratum was predominant in the earlier period, while strike-slip faulting was the main process during the later period (IGCEA, 1990; Zhang et al., 1991; Burchfiel et al., 1991; Wang et al., 2013b; Zhang et al., 2015).

In terms of tectonic deformations, the onset time for strike-slip faulting at the inner boundaries of the sub-blocks was close to that of the thrusting or fold deformation of the faults at the outer boundaries. For example, the Haiyuan fault (the inner boundary of the Tianjingshan block) transformed from thrusting to sinistral strike slip at approximately 5.4 Ma, at the same time whem the Tianjingshan fault (the outer boundary of the same block) began thrusting (Wang et al., 2013b). Furthermore, at approximately 2.6 or 2.7 Ma, the Tianjingshan fault (the inner boundary of the Yantongshan-Niushoushan block) transformed from thrusting to sinistral strike-slip (Wang et al., 2013b), meanwhile the vicinity of the SGK-NSSF (the outer boundary of the same block) was being compressed, which initiated fold deformation. Such a scenario, in which there was temporal synchronicity of tectonic deformations happening at different boundary faults of the same block but through different methods, could not possibly be coincidental. Instead, these were related to the inner sub-blocks being obstructed while pushing outward, resulting in lateral extrusion (Figure 10).

Specifically, the Nanhuashan-Liupanshan block was being compressed by the main Tibet Plateau block at approximately 10 Ma and commenced activities in the northeastern direction (Zheng et al., 2006; Wang et al., 2013a, 2013b). The Haiyuan fault, which forms the boundary between those two blocks, was obstructed by the Xiangshan-Tianjingshan block on the outside, and began thrusting activities (Figure 10c). At approximately 5.4 Ma (Wang et al., 2013b), given the sustained external compression by the Nanhuashan-Liupanshan sub-block, compression action on the Tianjingshan block became stronger. At the same time, it became more and more difficult for the Nanhuashan-Liupanshan block to maintain its activities in the northeastern direction. When the stalemate between the blocks reached a critical state, the Tianjingshan block began its northeastward extension, while the Nanhuashan-Liupanshan block acted toward the east, where obstruction forces were weaker. In so doing, a new equilibrium between the different activities was achieved (Figure 10b). Similarly, at approximately 2.7 or 2.6 Ma, sustained compression of the Tianjingshan block on the Yantongshan-Niushoushan block destroyed the inter-block equilibrium. Consequently, the affected blocks underwent similar adjustments, as described previously. Specifically, the Yantongshan-Niushoushan block began its northeastward extension, causing fold deformation and shortening (Wang et al., 2013b). At the same time, the Tianjingshan block began its activities towards the east, because the obstruction forces there were weaker (Figure 10c).

During the early Quaternary, the outer boundary of the Yantongshan-Niushoushan block did not exhibit any arcuate protrusion in the northeastern direction. Concurrently, the Yinchuan Basin, was affected by the counterclockwise rotation of the Ordos block (Zhang et al., 1998, 1999; Li et al., 2001; Zhang et al., 2006; Li et al., 2005). Thus, the block was no longer able to withstand the changes caused by the other blocks undergoing similar states of activities. Under the combined actions of the Tianjingshan block compressing toward the northeastern direction and the counterclockwise rotation of the Ordos block, the movement of this block was rapidly altered from activities in a northeastern direction to extrusion toward the northwest. This resulted in the dextral strike-slip faulting of the SGK-NSSF zone (Figure 10d).

It can thus be concluded that the extension of the arc tectonic belt in the northeastern margin of the Tibet Plateau was caused by the successive outward compression of the sub-blocks of the Tibet Plateau. The activities status of these sub-blocks controlled the nature of the activities at the boundary faults. It was the obstruction and subsequent lateral extrusion of the sub-blocks that resulted in the changes to the conditions of the boundary fault zones.

5. Conclusions

The SGK-NSSF is presently the foremost boundary of the arc tectonic belt extension in the northeastern margin of the

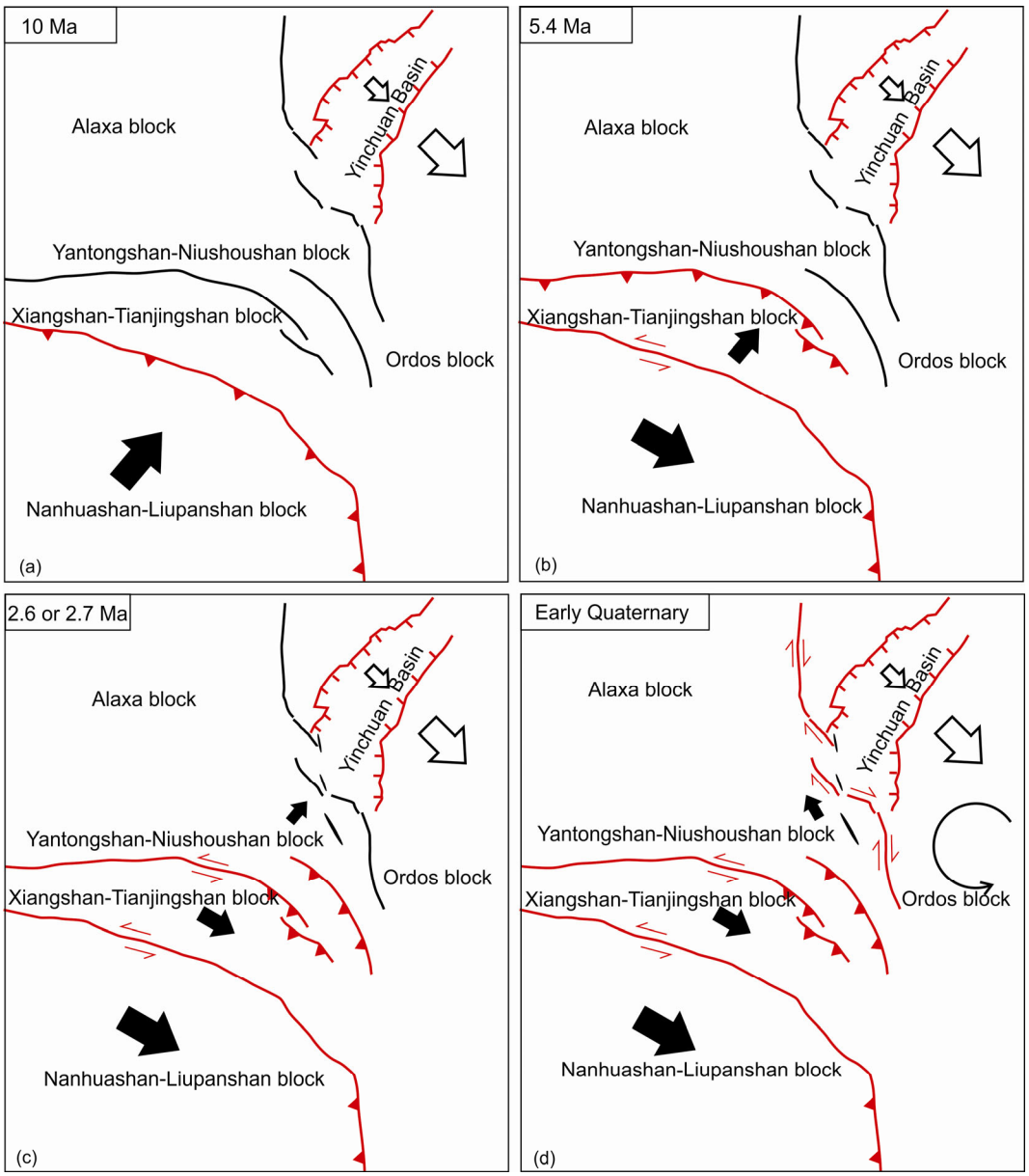

Figure 10 Model for extension of sub-blocks within the arc tectonic belt in the northeastern margin of the Tibet Plateau.

Tibet Plateau. It is a dextral strike-slip shear belt formed by three discontinuous secondary faults. The dextral strike-slip of the SGK-NSSF started at approximately the beginning of the Quaternary. It is a Holocene active fault with a maximum horizontal strike-slip displacement of 961 m, a horizontal strike-slip rate of about 0.35 mm/a during the late Quaternary, and coseismic horizontal displacement of approximately 3 m. The SGK-NSSF experienced two periods of tectonic deformation processes. The earlier period was predominantly stratigraphic fold deformation that was manifested as shortening of the sub-blocks and regional uplift, which was transformed into dextral strike-slip of the fault during the later period that was manifested as lateral extrusion of the sub-blocks. The timing of the two tectonic deformation periods was quite close: fold deformation occurred during the late Pliocene nearing 2.7 Ma, while faulting might have happened at the beginning of the Quaternary.

During the late Pliocene (~2.7 Ma), the extension of the Tibet Plateau reached the vicinity of the SGK-NSSF. The latter began undergoing dextral strike-slip at approximately the beginning of the Quaternary as a result of the combined actions of the northeastern compression of the Tibet Plateau and the counterclockwise rotation of the Ordos block. The extension of the arc tectonic belt in the northeastern margin of the Tibet Plateau was achieved through successive outward compression by the sub-blocks that occurred in stages. The margin reached the Haiyuan fault, Tianjingshan fault, and SGK-NSSF at 10, 5.4, and 2.7 Ma, respectively. The activity status of the sub-blocks controlled the nature of the activities at the boundaries and faults, with lateral extrusion

happening when the sub-blocks were obstructed. This was the root cause behind changes to the nature of the boundary fault zones.

Acknowledgements *We are grateful to Profs. Ran Yongkang, Zheng Dewen, Li Chuanyou, Ren Zhikun, Zhang Zhuqi, and Wu Chuanyong for guidance with fieldwork and valuable suggestions; to Prof. Wang Xulong, Dr. Du Jinhua and Xu Hongqiang for their help with dating of OSL samples; to the reviewers for their helpful advice and comments. This research was supported by the Fundamental Research Funds in Institute of Geology, China Earthquake Administration (Grant No. IGCEA1220), Special Project on Earthquake Research (Grant No. 201308012), National Natural Science Foundation of China (Grant Nos. 41202158, 41372220 & 41590861) and Science for Earthquake Resilience (Grant No. XH14052).*

References

Burchfiel B C, Deng Q D, Molnar P, Royden L, Wang Y P, Zhang P Z. 1989. Intracrustal detachment within zones of continental deformation. Geology, 17: 748–752

Burchfiel B C, Zhang P Z, Wang Y P, Zhang W Q, Song D M, Deng Q D, Molnar P, Royden L. 1991. Geology of the Haiyuan Fault zone, Ningxia Hui Autonomous Region, China, and its relation to the evolution of the northeastern margin of the Tibetan Plateau. Tectonics, 10: 1091–110

Chai C Z, Zhang W Q, Jiao D C. 1998. Quaternary structure feature in forward area of Tianjingshan fault (in Chinese). Earthq Res Chin, 14: 150–56

Chai C Z, Meng G K, Ma G R. 2011. Active Faults Exploration and Seismic Hazard Assessment in Yinchuan City (in Chinese). Beijing: Science Press. 28–30

Chen H, Hu J M, Gong W B, Li L B. 2013. Cenozoic deformation and evolution of the Niushoushan-Luoshan fault zone in the northeast margin of the Tibet Plateau (in Chinese). Earth Sci Front, 20: 018–035

Deng Q D, Sung F M, Zhu S L, Li M L, Wang T L, Zhang W Q. 1984. Active faulting and tectonics of the Ningxia-Hui autonomous region, China. J Geophy Res, 89: 4427–4445

Deng Q D, Liao Y H. 1996. Paleoseismology along the range-front fault of Helan Mountains, North Central China. J Geophys Res, 101: 5873–5894

Deng Q D, Zhang W Q, Zhang P Z, Jiao D C, Song F M, Wang Y P, Burchfiel B C, Molnar P, Royden L, Zhu S F, Zhu S L, Chai C Z. 1989. Haiyuan Strike slip Fault zone and its compressional structures of the end (in Chinese). Seismol Geol, 11: 1–14

Deng Q D, Zhang P Z, Ran Y K, Yang X P, Min W, Chu Q Z. 2003. Basic characteristics of active tectonics of China. Sci China Ser D-Earth Sci, 46: 356–372

England P, Houseman G. 1985. Role of lithospheric strength heterogeneities in the tectonics of Tibet and neighbouring regions. Nature, 315: 297–301

England P, Molnar P. 1997. The field of crustal velocity in Asia calculated from Quaternary rates of slip on fault. Geophys J Int, 130: 551–582

Jiang H C, Ding Z L, Xiong S F. 2007. Magnetostratigraphy of the Neogene Sikouzi section at Guyuan, Ningxia, China. Palaeogeography, 243: 223–234

Huo F C, Pan X S, You G L. 1989. Introduction to Geology of Ningxia (in Chinese). Beijing: Science Press.1–300

Institute of Geology, China Earthquake Administration (IGCEA), Earthquake Administration of Ningxia Hui Autonomous Region. 1990. Haiyuan Active Fault Zones (in Chinese). Beijing: Seismological Press. 1–278

Lei Q Y, Chai C Z, Meng G K, Du P, Wang Y, Xie X F. 2008. Composite drilling section exploration of Yinchuan buried fault (in Chinese). Seismol Geo, 30: 250–262

Lei Q Y, Chai C Z,Meng G K, Wang Y, Meng G K. 2011. Activity characteristics of Luhuatai buried fault since late Quaternary revealed by drilling (in Chinese). Seismol Geol, 33: 602–614

Lei Q Y, Chai C Z, Zheng W J, Du P, Xie X F, Wang Y, Cui J, Meng G K. 2014. Activity and slip rate in the northern section of the Yellow River fault by drilling (in Chinese). Seismol Geol, 36: 464–477

Li C Y, Zhang P Z, Yin J H, Min W. 2009. Late Quaternary left-lateral slip rate of the Haiyuan fault, northeastern marigin of the Tibetan Plateau. Tectonics, 28: 1–26

Li C Y. 2005. Quantitative studies on active faults in northeastern margins of the Tibetan Plateau (in Chinese). Ph D Thesis. Beijing: Institute of Geology, China Earthquake Administration. 1–150

Li K Q. 1992. Petroleum Geology of China (Vo1.12) (in Chinese). Beijing: Petroleum Industry Press. 362–371

Li Y X, Zhang J H, Guo L Q, Zhang Z F, Zhang J Q. 2005. Counter clock wise rotation and geodynamics of Ordos block (in Chinese). J Geog Geodyn, 25: 50–56

Li W L, Lu Y C, Ding G Y. 2001. Paleomagnetic evidence from loess for the relative motion between the Ordos and its adjacent blocks (in Chinese). Quat Sci, 21: 551–559

Liang H, Zhang K, Fu J L, Li Z B, Chen J, Lu K. 2013. The neotectonics in the Niushou Mountains, the northeastern margin of the Tibetan Plateau, China and its impact on the evolution of the Yellow River (in Chinese). Earth Sci Front, 20: 182–189

Liao Y H, Chai C Z, Zhang W X, Xu W J. 2000. The active features and slip rate of Lingwu faults in Late Quaternary (in Chinese). Earthq Res China, 16: 64–71

Liu J H, Zhang P Z, Zheng D W, Wan J L, Wang W T, Du P, Lei Q Y. 2010. Pattern and timing of late Cenozoic rapid exhumation and uplift of the Helan Mountain, China. Sci China Earth Sci, 53: 345–355

Molnar P, Tapponnier P. 1975. Cenozoic tectonics of Asia: effects of a continental collision. Science, 189: 4l9–426

Min W, Jiao D C, Chai C Z, Zhang P Z. 2003. Characteristics of the active Luoshan fault since late Pleistocene, north central China (in Italian). Anal Geofisi, 46: 997–1014

Min W, Chai C Z, Wang P, Yang P. 1992. Preliminary study on the Holocene active fault features at the eastern piedmont of the Luoshan Mountain (in Chinese). Earthq Res Chin, 8: 49–54

Ningxia Bureau of Geology and Mineral Resources (NBGMR). 1990. Regional geology of Ningxia Hui Autonomous Region (in Chinese). Beijing: Geological Publishing House. 65–440

Peltzer G, Tapponnier P, Armijo R. 1989. Magnitude of Quaternary left lateral displacements along the north edge of Tibet. Science, 246: 1285–1289

Shen X H, Tian Q J, Ding G Y, Wei K B, Chen Z W. 2001. The late Cenozoic stratigraphic sequence and its implication to tectonic evolution, Hejiakouzi area, Ninxia Hui Autonomous Region (in Chinese). Earthq Res China, 17: 156–165

Shi W, Liu Y, Liu Y, Chen P, Chen L, Cen M, Huang X F, Li H Q. 2013. Cenozoic evolution of the Haiyuan fault zone in the northeast margin of the Tibetan Plateau (in Chinese). Earth Sci Front, 20: 001–017

Scholz C H. 2002. The Mechanics of Earthquakes and Faulting. Cambridge: Cambridge University Press. 175–243

Tapponnier P, Peltzer G, Dain A Y, Armijo R, Cobbold P. 1982. Propagating extrusion tectonics in Asia: New insights from simple experiments with plasticine. Geology, 10: 611–616

Tapponnier P, Xu Z Q, Roger F, Meyer B, Arnaud N, Wittlinger G, Yang J S. 2001. Oblique stepwise rise and growth of the Tibet Plateau. Science, 294: 1671–1677

Tang X Y, Feng Q, Li D S. 1990. Tectonic characteristics and evolution of Bayanhot basin, western Inner Mongolia (in Chinese). Oil Gas Geol, 11: 127–135

The Research Group on Active Fault Systems around the Ordos Massif (RGAFSAO). 1988. Active Fault System Around Ordos Massif (in Chinese). Beijing: Seismological Press. 28–30

Wang W T, Zhang P Z, Lei Q Y. 2013a. Deformational characteristics of the Niushoushan-Luoshan fault zone and its tectonic implications (in Chinese). Seismol Geol, 35: 1–13

Wang W T, Kirby E, Zhang P Z, Zhen D W, Zhang G L, Chai C Z. 2013b. Tertiary basin evolution along the northeastern margin of the Tibetan plateau: Evidence for basin formation during Oligocene transtension.

Geol Soc Am Bull, 142: 113–137
Wang W T, Zhang P Z, Kirby E, Wang L H, Zhang G L. 2011. A revised chronology for Tertiary sedimentation in the Sikouzi Basin: Implications for the tectonic evolution of the northeastern corner of the Tibetan plateau. Tectonophysics, 505: 100–114
Wang W T, Zhang P Z, Zheng D W, Pang J Z. 2014. Late Cenozoic tectonic deformation of the Haiyuan fault zone in the northeastern of Tibetan Plateau (in Chinese). Earth Sci Front, 21:266–274
Xu X W, Wen X Z, Ye J Q, Ma B Q, Chen J, Zhou R J, He H L, Tian Q J, He Y L, Wang Z C, Sun Z M, Feng X J, Yu G H, Chen L C, Chen G H, Yu S E, Ran Y K, Li X G, Li C X, An Y F. 2008. The *M*s8.0 Wenchuan earthquake surface ruptures and its seismogenic structure (in Chinese). Seismol Geol, 30: 597–629
Yan L H, Wang L. 2002. Geo-thermal Resources in Yinchuan Basin (in Chinese). Yinchuan: Ningxia People Press. 1–169
Zhang J, Ma Z J, Ren W J. 2004. The tectonic characteristics of southern Helan Mountain and their relationships with the Guyuan-Qingtongxia fault (in Chinese). J Jinlin Univ (Earth Sci Ed), 34: 187–205
Zhang J, Cunningham D, Chen H Y. 2010. Sedimentary characteristics of Cenozoic strata in central-southern Ningxia, NW China: Implications for the evolution of the NE Qinghai-Tibetan plateau. J Asian Earth Sci, 39: 740–749
Zhang P Z, Deng Q D, Zhang G M, Ma J, Gan W J, Min W, Mao F Y, Wang Q. 2003. Active tectonic blocks and strong earthquakes in the continent of China. Sci China Ser D-Earth Sci, 46 (Suppl 1):13–24
Zhang P Z, Deng Q D, Zhang Z Q, Li H B. 2013. Active faults, earthquake hazards and associated geodynamic processes in continental China (in Chinese). Sci China Earth Sci, 43: 1607–1620
Zhang P Z, Molnar P, Burchfiel B C, Royden L, Wang Y P, Deng Q D, Song F M, Zhang W Q, Jiao D C. 1988. Bounds on the Holocene slip rate along the Haiyuan fault, north-central China. Quaternary Res, 30: 151–164
Zhang P Z, Burchiel B C, Molnar P, Zhang W Q, Jiao D C, Deng Q D, Wang Y P, Royden L, Song F M. 1990. Late Cenozoic tectonic evolution of the Ningxia-Hui Atonomous Region, China. Geol Soc Am Bull, 102: 1484–1498
Zhang P Z, Burchfiel B C, Molnar P, Zhang W Q, Jiao D C, Deng Q D, Wang Y P, Royden L, Song F M. 1991. Amount and style of late Cenozoic deformation in the Liupan Shan area, Ningxia Autonomous Region, China. Tectonics, 10: 1111– 1129
Zhang P Z, Shen Z K, Wang M, Gan W J, Bürgmann R, Molnar P. 2004. Continuous deformation of the Tibetan Plateau from Global Positioning System date. Geology, 32: 809–812
Zhang Y Q, Liao C Z, Shi W, Hu B. 2006. Neotectonic evolution of the peripheral zones of the Ordos Basin and geodynamic setting (in Chinese). Geol J Chin Univ, 12: 285–297
Zhang Y Q, Mercier J L, Vergely P. 1998. Extension in the graben systems around the Ordos (China), and its contribution to the extrusion tectonics of south China with respect to Gobi-Mongolia. Tectonophysics, 285: 41–75
Zhang Y Q, Vergely P, Mercier J L. 1999. Pliocene-Quaternary faulting pattern and left-slip propagation tectonics in North China. Episodes, 22: 84–88
Zhang W Q, Jiao D C, Chai C Z. 2015. Tianjingshan Active Fault (in Chinese). Beijing: Seismological Press. 1–270
Zheng D W, Zhang P Z, Wan J L, Yan D Y, Zhang G L, Li C Y. 2005. Apatite fission track evidence for the thermal history of the Liupanshan basin (in Chinese). Chin J Geophys, 48: 157–164
Zheng D W, Zhang P Z, Wan J L. 2006. Rapid exhumation at ~8 Ma on the Liupan Shan thrust fault from apatite fission-track thermochronology: Implications for growth of the northeastern Tibetan plateau margin. Earth Planet Sci Lett, 248: 198–208
Zheng W J, Zhang P Z, Yuan D Y, Zhen D W. 2009. Deformation on the northern of the Tibetan plateau from GPS measurement and geologic rates of late Quaternary along the major fault (in Chinese). Chin J Geophys, 52: 2491–2508
Zheng W J, Zhang P Z, Zhang, Ge W P, Molnar P, Zhang H P. 2013a. Late Quaternary slip rate of the South Heli Shan Fault (northern Hexi Corridor, NW China) and its implications for northeastward growth of the Tibetan Plateau. Tectonics, 32: 271–293
Zheng W J, Zhang H P, Zhang P Z, Molnar P, Liu X W, Yuan D Y. 2013b. Late Quaternary slip rates of the thrust faults in western Hexi Corridor (Northern Qilian Shan, China) and their implications for northeastward growth of the Tibetan Plateau. Geosphere, 9: 342–354